Low Sidelobe Level Millimeter-Wave Asymmetric Bull's Eye Antenna with Minimal Profile Feeding

Miguel Navarro-Cía, *Senior Member, IEEE*, Unai Beaskoetxea, Jorge Teniente and Miguel Beruete

***Abstract*—Bull's eye antennas exhibit remarkable directivity considering their low profile, albeit accompanied by high sidelobes. This undesirable radiation characteristic is tackled here by reporting a complementary split ring feeding whereby the broadside space-wave partially responsible for the high sidelobes is cancelled while the leaky-wave is excited effectively. This feeding results into an asymmetric bull's eye antenna with minimal profile ($\sim$0.73λ_0) and no protrusions on the radiating interface. The fabricated 10 period antenna operating in the Ka band shows a directivity of 23.5 dBi, a sidelobe level of -22.9 dB (>6 dB improvement compared to other bull's eye antennas) and a beamwidth of 3.7° and 6.7° in the E- and H-plane, respectively.**

***Index Terms*—Bull's eye antenna, leaky-wave antenna, millimeter-waves, Ka-band.**

I. Introduction

BULL's eye antennas have become the subject of intensive research because of their low profile and moderate directivity [1]. Its microstrip implementation [2]–[4] outperforms the metal corrugated counterpart [5] for microwave applications due to its lightweight and reconfigurability through a complex feeding system not suitable for the metal corrugated approach [6]. However, for frequencies beyond K band, dielectric losses in microstrip technology make metal corrugated bull's eye antennas the preferred option [7]–[18].

A challenge that bull's eye antennas face is their high sidelobes due to the interference of the direct space-wave radiation through the slot with the leaky-wave mode radiation sustained by the corrugations [19]. To address this issue in a microstrip-implemented bull's eye antenna, previous studies [20], [21] introduced a monopole feeding technique, exploiting the fact that an ideal monopole has a null at broadside (i.e., monopole's axis) and most of the power is directed in the transverse direction. However, this solution not only impacts negatively on the profile of the antenna given the protrusion on the radiating interface, but also its performance deteriorates at high frequencies such as millimeter-waves. An alternative solution proposed for millimeter-wave metal corrugated bull's eye antennas involves utilizing the second higher order mode of a circular waveguide (the transverse magnetic, TM, TM_{01} mode) feed [16]. However, the whole antenna, including the feeding network, is no longer low profile.

In this Letter, we propose a complementary split ring feeding (i.e., double slot) to maintain the low profile of the bull's eye antenna while reducing sidelobe levels (SLL). The double slot was introduced successfully for leaky-wave lens antennas [22]–[24], operating as an iris with both slots in phase, leading to effective in-plane magnetic and electric dipole moments that prevent the excitation of the undesired TM_0 mode supported by the dielectric-air-ground plane cavity. Here, we exploit the fundamental resonance of the double slot whereby the

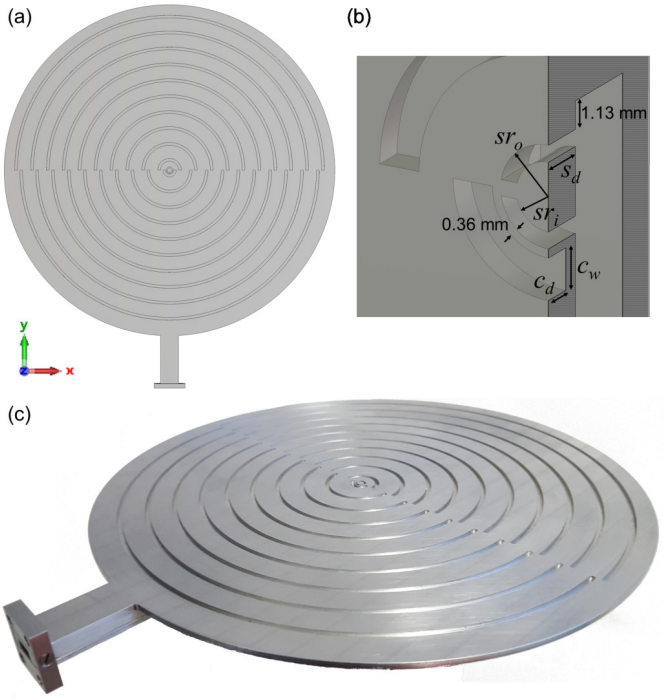

Fig. 1. (a) Sketch of the bull's eye antenna, including waveguide feeding. (b) Detail of the double slot with a cutting plane normal to $x = 0$. (c) Photograph of the fabricated antenna made of aluminium.

This work was supported in part by the Engineering and Physical Sciences Research Council (EPSRC) [Grant No. EP/S018395/1], and in part by the Spanish "Ministerio de Ciencia e Innovación (MCIN)" and the Spanish "Agencia Estatal de Investigación (AEI)" (MCIN/AEI/10.13039/501100011033/FEDER "Una manera de hacer Europa") through Project Number RTI2018-094475-B-I00. The work of M. Navarro-Cía was supported by the Royal Society [Grant No. RSG/R1/180040], and the University of Birmingham [Birmingham Fellowship]. For the purpose of open access, the author(s) has applied a Creative Commons Attribution (CC BY) license to any Accepted Manuscript version arising. (*Corresponding author: Miguel Navarro-Cía*)

M. Navarro-Cía is with the School of Physics and Astronomy, and the Department of Electronic, Electrical and System Engineering, University of Birmingham, Birmingham B15 2TT, United Kingdom (e-mail: M.Navarro-Cia@bham.ac.uk).

U. Beaskoetxea is with Anteral S.L., Edificio I+D "Jerónimo de Ayanz", Campus Arrosadía 31006 Pamplona, Spain (e-mail: ubeaskoetxea@anteral.com).

J. Teniente and M. Beruete are with the Antennas Group, and the Institute of Smart Cities (ISC), Universidad Pública de Navarra, 31006 Pamplona, Spain (e-mails: jorge.teniente@unavarra.es, miguel.beruete@unavarra.es).

slots are out of phase, yielding instead an effective in-plane magnetic dipole moment, m_x, and an out-of-plane electric dipole moment, p_z, [25], [26] that ensure a null at broadside and good coupling to the leaky-wave akin to the monopole or the TM_{01} mode feeding approaches. Unlike the monopole [20], [21] and TM_{01} mode [16] feeding approaches, it does not have any impact in the overall profile of the antenna. An antenna operating at the Ka-band is designed, fabricated (see Fig. 1) and measured to demonstrate the simplicity, yet effectiveness of the double slot feeding.

II. Antenna Design and Initial Numerical Results

Similar to the monopole feeding, an asymmetric (with respect to the *xz*-plane) bull's eye antenna needs to be designed to have in-phase radiation from both halves. The final dimensions of the 10 period antenna operating at ∼29 GHz (see dispersion characteristic of the leaky-wave mode for the corresponding infinite 1D corrugated metal plane in Fig. 2) can be found in Table I and were obtained after mesh convergence analysis and optimisation using the CST Microwave Studio^{TM} in-built Trust Region Framework algorithm. The seed dimensions for the corrugations followed the design guidelines found elsewhere [1], [12], [20], and in short are $p = \lambda_0$, $c_d = \lambda_0/4$ and $c_w << \lambda_0$; the initial distance between the double slot centre and the feeding waveguide end was $0.4\lambda_g$, where λ_g is the guided wavelength, akin to waveguide to coaxial transitions. Notice that the total antenna thickness corresponds to standard WR-28 waveguide flange (UG-599/U MOD flange); otherwise, the antenna thickness is constrained by the amplitude of the corrugation c_d and the outer dimensions of the WR-28 waveguide, resulting into 7.56 mm $\sim 0.73\lambda_0$.

TABLE I
Antenna Dimensions

Parameter	Dimensions (mm)
Period, p	9.85
Corrugation width, c_w	1.70
Corrugation depth, c_d	1.30
offset 1, o_1	6.45
offset 2, o_2	3.28
Slot outer diameter, $2sr_o$	4.13
Slot inner diameter, $2sr_i$	2.77
Slot depth, s_d	2.00
Total antenna diameter (excluding feeding)	204.90
Waveguide feeding length (excluding flange)	137.20
Total thickness (excluding flange)	7.56

The antenna feeding includes a standard waveguide (WR-28, Ka-band) that runs along the back of the indented plate and the double slot (Fig. 1(a,b)). The power is coupled to the output by means of the double slot transverse resonance (see insets in Fig. 3(a) demonstrating p_z and that the slots' E-fields are out-of-phase), which is highly affected by the distance from the center of the antenna (i.e., the double slot position) to the first corrugations, as demonstrated by the S_{11} shown in Fig. 3(a). This double-slot-centre to first-corrugation-centre distance, which we referred to as offset, has also an impact on the coupling efficiency to the leaky-wave mode. Choosing the distance (i.e., offset) equal to the grating period

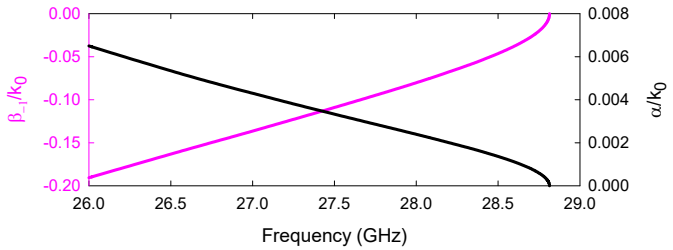

Fig. 2. Dispersion characteristic of the leaky-wave mode on an infinite 1D model of the proposed leaky-wave antenna, determined using the general lossy method of the eigenmode solver of CST Microwave Studio^{TM}. The attenuation (leakage) constant α was computed from the quality factor (Q) of the leaky-wave mode through the relationship $\alpha = \beta_{-1}/2Q$.

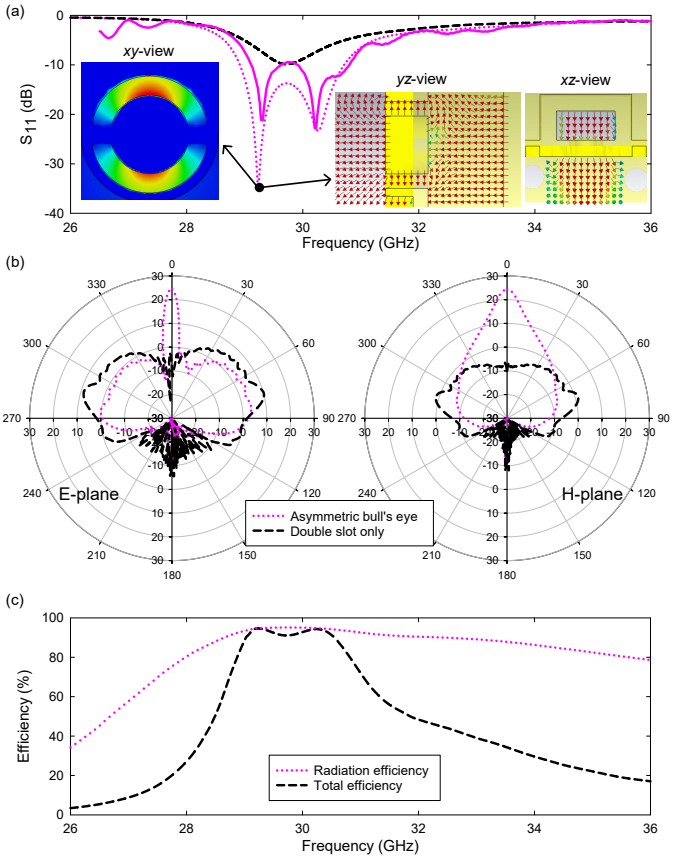

Fig. 3. (a) Simulated S_{11} for the bull's eye (dotted pink) and double slot only antenna (dashed black), and measured S_{11} (solid pink). Insets: from left to right, $Max(E_{tang})$ on the xy cross section inside the double slot, and E-field distribution on the yz-plane and xz-plane. (b) Far field radiation pattern in polar coordinates with directivity values in dBi on the E-plane and H-plane for the the bull's eye (dotted pink) and double slot only antenna (dashed black). (c) Simulated radiation and total efficiency of the asymmetric bull's eye antenna.

is usually not optimal owing to the intense reactive field around a metallic aperture [27]. After optimisation, we obtained the offsets o_1 and o_2 tabulated in Table I. The radiation pattern at the S_{11} minimum with and without corrugations is plotted in Fig. 3(b) to demonstrate the null at almost broadside for the double slot alone. Note that the null is not exactly at broadside in the E-plane due to slight asymmetric excitation of the

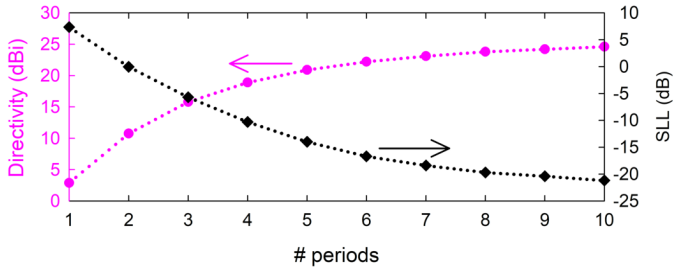

Fig. 4. Evolution of the directivity (pink circle) and SLL (black diamond) as a function of the number of periods on a 204.9 mm diameter aluminium plate.

double slot (see left inset in Fig. 3(a)), which in turn yields a minimum in the H-plane less marked than that of the E-plane for the double slot alone. The asymmetric bull's eye antenna radiates at broadside despite the open stopband condition whereby $\alpha = 0$ at exactly broadside (see Fig. 2) because each half radiates to an appropriate scan angle slightly away from the broadside direction that results into a maximum power density in the broadside direction [28]; in addition, the open stopband condition is smeared out because the asymmetric bull's antenna is not an ideal periodic structure of infinite length. The asymmetric bull's eye antenna directivity, D, at broadside is 24.5 dBi and the corresponding realised gain is 24.3 dBi. Notice that the SLL is better than -20 dB for the asymmetric bull's eye antenna. The simulated radiation and total efficiency of the final asymmetric design can be found in Fig. 3(c); they both reach 94.8% at the S_{11} minimum.

Figure 4 shows the evolution of the broadside directivity and SLL at the design frequency for an increasing number of periods. When the number of periods is small, a leaky-wave is not supported yet and the corrugations act as simple parasitic elements. Hence, the directivity is lower and the main angle of radiation is not at broadside, leading to positive SLL. Beyond 3 periods, the leaky-wave develops in the corrugations and the broadside directivity increases asymptotically due to the leaky-wave contribution, while the SLL decreases also asymptotically. The values of directivity achieved are moderate when compared to parabolic reflectors and reflectarrays of the same diameter, but the latter antennas have the feed at a distance approximately 0.6 times their diameter. Higher directivity, and thus, aperture efficiency, than that reported here is possible in bull's eye antennas by tapering the modulated surface reactance [16].

III. Fabricated Prototype and Discussion

To ease fabrication with a three-axis computer numerical control milling machine, the prototype was split into three blocks (noticeable in Fig. 1(c)): one block includes the aluminum plate with indented rings and a double slot on the top surface as well as the top and lateral walls of the feeding waveguide; the bottom lid of the feeding waveguide and the flange form each of them a single machined block. The H-plane split approach is used here since an E-plane split would affect the double slot feeding and the leaky-wave mode. The split is judiciously at the bottom of the H-plane where

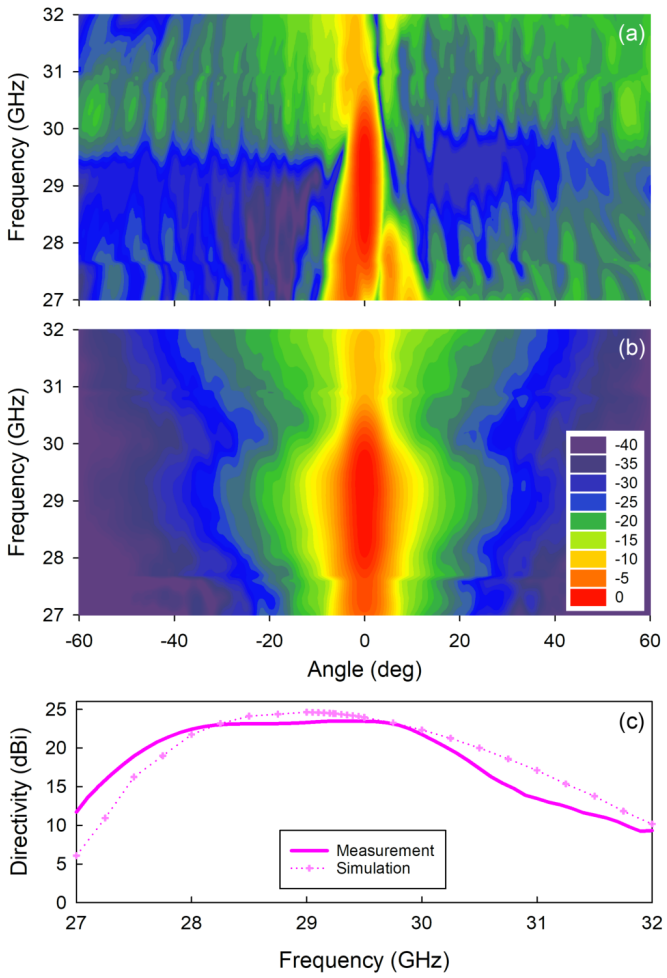

Fig. 5. Measured co-polar radiation pattern spectrum in the E-plane (a) and H-plane (b). Note that both colormaps share the same colorbar. Broadside directivity (c): measured (solid line) and simulated data (symbol-dotted line).

the surface current are lower to minimise losses [29]. All aluminium blocks were joined back together with screws in counterbore holes. Note that the asymmetric design does not offer an advantage or disadvantage compared to a symmetric design given the characteristics of computer numerical control milling machining.

The prototype was measured in a planar near field facility employing a WR-28 open ended waveguide probe with sharpened edges to minimize reflections. The measured S_{11} is shown in Fig. 3(a) and agrees well with the numerical calculations, albeit some degradation in performance is noticeable, which we attribute to imperfect electrical contact between the different split blocks. The bull's eye normalized far field radiation pattern as a function of angle and frequency for both E- and H-planes is mapped in Fig. 5(a,b). The measured directivity peak value is 23.5 dBi at 29.4 GHz. The directivity bandwidth, considering a 3 dB reduction in directivity compared to the peak value, spans from 27.6 to 30.2 GHz. Simulated and measured results agree well, see Fig. 5(c). The increase in directivity is achieved by the in-phase radiation from the corrugations that is realised through the asymmetric

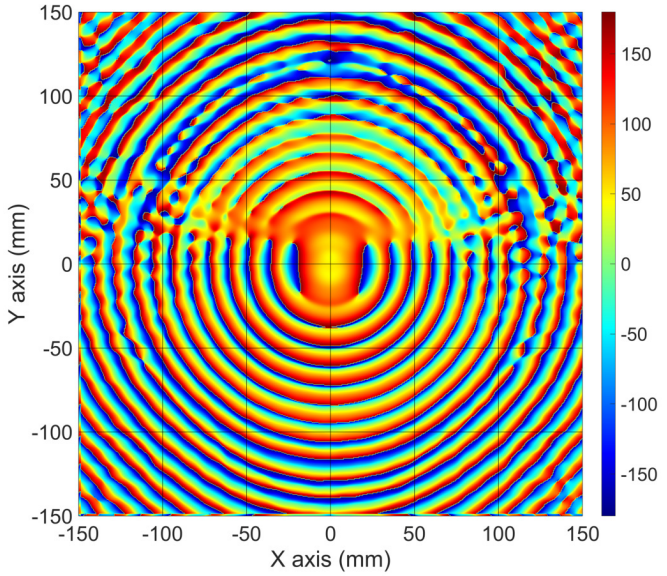

Fig. 6. Measured phase of the co-polar near-field distribution at 29.4 GHz.

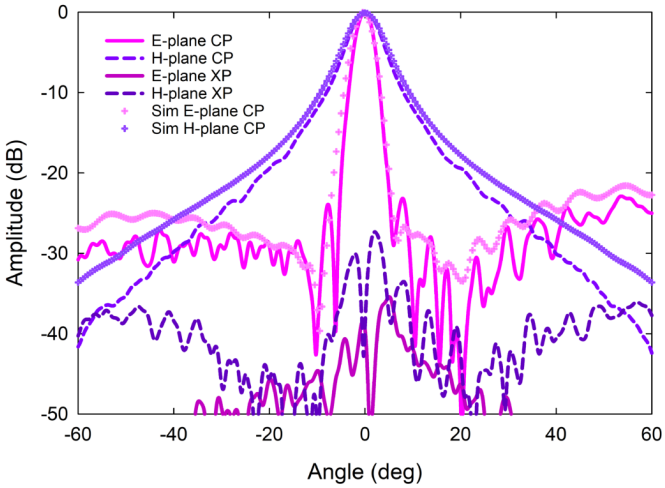

Fig. 7. Normalized radiation pattern at 29.4 GHz for both E- (pink) and H-planes (purple): co-polar (light color) and cross-polar (dark color). Measurements and simulation data are plotted with lines and symbols, respectively. The latter is only plotted for the co-polar component.

bull's eye implementation, as demonstrated by the measured phase of the co-polar aperture field in Fig. 6. We attribute the difference in directivity between measurement and simulation to fabrication tolerances. The E-plane colormap reveals the n = -1 leaky-wave modes propagating along the corrugations whose angles of radiation merge at broadside at 29.4 GHz. At this frequency, the SLL is -22.9 dB, which outperforms any bull's eye antenna reported in the literature with similar number of periods as illustrated in Table II. There are no signs of the n = -2 leaky-wave modes within the frequency-angle range displayed.

TABLE II
COMPARISON WITH THE LITERATURE - MEASURED DATA

Param.	**[3]**	**[4]**	**[5]**	**[6]**	**[9]**	**[15]**	**[20]**	**Here**
f (GHz)	21.2	19.5	16.5	19.9	60	96	13	29.4
Periods	14	10	6	10	6	7	5	10
SLL (dB)	-10	-15	-14	-10	-14	-10.8	-16	-22.9
D (dBi)	26	-	-	-	-	-	-	23.5
G (dBi)	-	17	23	10	19	17	19	-
A_e (%)	28	3	9	1	2	6	9	6

A disadvantage of bull's eye antennas is their low aperture efficiency (A_e) as Table II illustrates. For the antenna reported in this work, A_e = 6%; only the use of a high permittivity dielectric in a microstrip implementation allows a moderate value of A_e [3]. This is resolved with radial-line slot array antennas that can obtain aperture efficiencies as high as 82% with gain ranging from approximately 30 to 35 dBi [30]–[34]. However, these antennas still face SLL in the range of -15 dB, their design and fabrication is complex, and their multi-layer structure yield thick antennas.

To facilitate the comparison with simulation, a frequency cut at the peak of directivity is singled out from the colormaps and plotted together with the simulated radiation pattern in Fig. 7. One can observe a good agreement with a minor deviation in the H-plane. This deviation is arguably due to fabrication tolerances in the double slot as it plays the major role in the H-plane. The cross-polar radiation pattern is also plotted in Fig. 7 for completeness. By virtue of the magnetic symmetry in the E-plane, the measured cross-polar at broadside is very low (ideally, it is a null) and remains below -27.3 dB in both E- and H-planes. The measured beamwidth is 3.7° and 6.7° for the E- and H-plane, respectively.

IV. CONCLUSION

To tackle the high sidelobe levels of bull's eye antennas, an asymmetric metal corrugated bull's eye antenna fed by a central double slot has been presented. The use of the double slot instead of the monopole feed recently reported to reduce sidelobe levels maintain the attractive low profile of the bull's eye antenna without any penalty in other radiation characteristics. The experimental results demonstrate a directive antenna of D = 23.5 dBi with SLL = -22.9 dB, which is at least 6 dB better than resonant rectangular slot fed and microstrip implemented bull's eye antennas. This antenna might be of interest for space applications above K-band where all-metallic antennas with low profiles are preferred even at the expense of directivity and aperture efficiency.

ACKNOWLEDGEMENTS

The authors would like to thank S. Brookes (University of Birmingham) for supporting the fabrication and Talal Skaik (University of Birmingham) for confirming S_{11} measurements with a Keysight N5245A vector network analyzer.

REFERENCES

[1] M. Beruete, U. Beaskoetxea, M. Zehar, A. Agrawal, S. Liu, K. Blary, A. Chahadih, X.-L. Han, M. Navarro-Cía, D. Etayo Salinas, A. Nahata, T. Akalin, and M. Sorolla Ayza, "Terahertz Corrugated and Bull's-Eye Antennas," *IEEE Transactions on Terahertz Science and Technology*, vol. 3, no. 6, pp. 740–747, 2013.

[2] P. Baccarelli, P. Burghignoli, G. Lovat, and S. Paulotto, "A novel printed leaky-wave 'bull-eye' antenna with suppressed surface-wave excitation," *IEEE Antennas and Propagation Society, AP-S International Symposium (Digest)*, vol. 1, pp. 1078–1081, 2004.

[3] S. K. Podilchak, A. P. Freundorfer, and Y. M. Antar, "Planar leaky-wave antenna designs offering conical-sector beam scanning and broadside radiation using surface-wave launchers," *IEEE Antennas and Wireless Propagation Letters*, vol. 7, pp. 155–158, 2008.

[4] S. K. Podilchak, P. Baccarelli, P. Burghignoli, A. P. Freundorfer, and Y. M. Antar, "Analysis and design of annular microstrip-based planar periodic leaky-wave antennas," *IEEE Transactions on Antennas and Propagation*, vol. 62, no. 6, pp. 2978–2991, 2014.

[5] M. Beruete, I. Campillo, J. S. Dolado, J. E. Rodríguez-Seco, E. Perea, F. Falcone, and M. Sorolla, "Very low-profile "bull's eye" feeder antenna," *IEEE Antennas and Wireless Propagation Letters*, vol. 4, no. 1, pp. 365–368, 2005.

[6] D. Comite, S. K. Podilchak, P. Baccarelli, P. Burghignoli, A. Galli, A. P. Freundorfer, and Y. M. Antar, "Design of a polarization-diverse planar leaky-wave antenna for broadside radiation," *IEEE Access*, vol. 7, pp. 28 672–28 683, 2019.

[7] T. Ishi, J. Fujikata, K. Marita, T. Baba, and K. Ohashi, "Si nano-photodiode with a surface plasmon antenna," *Japanese Journal of Applied Physics, Part 2: Letters*, vol. 44, no. 12-15, pp. 14–17, 2005.

[8] N. Yu, R. Blanchard, J. Fan, F. Capasso, T. Edamura, M. Yamanishi, and H. Kan, "Small divergence edge-emitting semiconductor lasers with two-dimensional plasmonic collimators," *Applied Physics Letters*, vol. 93, no. 18, pp. 18–21, 2008.

[9] C. J. Vourch and T. D. Drysdale, "V-band 'bull's eye' antenna for cubeSat applications," *IEEE Antennas and Wireless Propagation Letters*, vol. 13, pp. 1092–1095, 2014.

[10] U. Beaskoetxea, V. Pacheco-Peña, B. Orazbayev, T. Akalin, S. Maci, M. Navarro-Cía, and M. Beruete, "77-GHz High-Gain Bull's-Eye Antenna With Sinusoidal Profile," *IEEE Antennas and Wireless Propagation Letters*, vol. 14, 2015.

[11] Y. Monnai, D. Jahn, W. Withayachumnankul, M. Koch, and H. Shinoda, "Terahertz plasmonic Bessel beamformer," *Applied Physics Letters*, vol. 106, no. 2, 2015. [Online]. Available: http://dx.doi.org/10.1063/1.4905445

[12] U. Beaskoetxea, M. Navarro-Cía, and M. Beruete, "Broadband frequency and angular response of a sinusoidal Bull's-Eye," *Journal of Physics D: Applied Physics*, vol. 49, no. 26, pp. 265 103–1–6, 2016.

[13] C. J. Vourch, B. Allen, and T. D. Drysdale, "Planar millimetre-wave antenna simultaneously producing four orbital angular momentum modes and associated multi-element receiver array," *IET Microwaves, Antennas and Propagation*, vol. 10, no. 14, pp. 1492–1499, 2016.

[14] C. J. Vourch and T. D. Drysdale, "V-band Bull's eye antenna for multiple discretely steerable beams," *IET Microwaves, Antennas and Propagation*, vol. 10, no. 3, pp. 318–325, 2016.

[15] U. Beaskoetxea, S. Maci, M. Navarro-Cía, and M. Beruete, "3-D-Printed 96 GHz bull's-eye antenna with off-axis beaming," *IEEE Transactions on Antennas and Propagation*, vol. 65, no. 1, pp. 17–25, 2017.

[16] D. Gonzalez-Ovejero, N. Chahat, R. Sauleau, G. Chattopadhyay, S. Maci, and M. Ettorre, "Additive manufactured metal-only modulated metasurface antennas," *IEEE Transactions on Antennas and Propagation*, vol. 66, no. 11, pp. 6106–6114, 2018.

[17] D. Perez-Quintana, I. Ederra, and M. Beruete, "Bull's-Eye Antenna with Circular Polarization at Millimeter Waves Based on Ridge Gap Waveguide Technology," *IEEE Transactions on Antennas and Propagation*, vol. 69, no. 4, pp. 2376–2379, 2021.

[18] D. Kampouridou and A. Feresidis, "Broadband THz Corrugated Bull's Eye Antennas," *IEEE Access*, vol. 9, pp. 104 460–104 468, 2021.

[19] D. R. Jackson, P. Burghignoli, G. Lovat, F. Capolino, J. Chen, D. R. Wilton, and A. A. Oliner, "The fundamental physics of directive beaming at microwave and optical frequencies and the role of leaky waves," *Proceedings of the IEEE*, vol. 99, no. 10, pp. 1780–1805, 2011.

[20] U. Beaskoetxea, A. E. Torres-Garcia, and M. Beruete, "Ku-Band Low-Profile Asymmetric Bull's-Eye Antenna with Reduced Sidelobes and Monopole Feeding," *IEEE Antennas and Wireless Propagation Letters*, vol. 17, no. 3, pp. 401–404, 2018.

[21] D. Comite, V. G. G. Buendia, S. K. Podilchak, D. D. Ruscio, P. Baccarelli, P. Burghignoli, and A. Galli, "Planar antenna design for omnidirectional conical radiation through cylindrical leaky waves," *IEEE Antennas and Wireless Propagation Letters*, vol. 17, no. 10, pp. 1837–1841, 2018.

[22] N. Llombart, G. Chattopadhyay, A. Skalare, and I. Mehdi, "Novel terahertz antenna based on a silicon lens fed by a leaky wave enhanced waveguide," *IEEE Transactions on Antennas and Propagation*, vol. 59, no. 6, pp. 2160–2168, 2011.

[23] D. Blanco, N. Llombart, and E. Rajo-Iglesias, "On the use of leaky wave phased arrays for the reduction of the grating lobe level," *IEEE Transactions on Antennas and Propagation*, vol. 62, no. 4, pp. 1789–1795, 2014.

[24] D. Blanco, E. Rajo-Iglesias, S. Maci, and N. Llombart, "Directivity enhancement and spurious radiation suppression in leaky-wave antennas using inductive grid metasurfaces," *IEEE Transactions on Antennas and Propagation*, vol. 63, no. 3, pp. 891–900, 2015.

[25] Y. U. Lee, J. Kim, and J. W. Wu, "Electro-optic switching in metamaterial by liquid crystal," *Nano Convergence*, vol. 2, no. 1, pp. 0–7, 2015.

[26] P. Rodríguez-Ulibarri and M. Beruete, "Nonbianisotropic complementary split ring resonators as angular selective metasurfaces," *Journal of the Optical Society of America B*, vol. 34, no. 7, p. D56, 2017.

[27] N. Yu, Q. J. Wang, C. Pflügl, L. Diehl, F. Capasso, T. Edamura, S. Furuta, M. Yamanishi, and H. Kan, "Semiconductor lasers with integrated plasmonic polarizers," *Applied Physics Letters*, vol. 94, no. 15, 04 2009, 151101.

[28] D. R. Jackson, A. A. Oliner, T. Zhao, and J. T. Williams, "Beaming of light at broadside through a subwavelength hole: Leaky wave model and open stopband effect," *Radio Science*, vol. 40, no. 6, 2005.

[29] B. Beuerle, J. Campion, U. Shah, and J. Oberhammer, "A Very Low Loss 220–325 GHz Silicon Micromachined Waveguide Technology," *IEEE Transactions on Terahertz Science and Technology*, vol. 8, no. 2, pp. 248–250, 2018.

[30] J. M. Fernandez Gonzalez, P. Padilla, G. Exposito-Dominguez, and M. Sierra-Castaner, "Lightweight portable planar slot array antenna for satellite communications in x-band," *IEEE Antennas and Wireless Propagation Letters*, vol. 10, pp. 1409–1412, 2011.

[31] A. Tamayo-Domínguez, J.-M. Fernández-González, and M. Sierra-Castañer, "Monopulse radial line slot array antenna fed by a 3-d-printed cavity-ended modified butler matrix based on gap waveguide at 94 ghz," *IEEE Transactions on Antennas and Propagation*, vol. 69, no. 8, pp. 4558–4568, 2021.

[32] M. N. Y. Koli, M. U. Afzal, K. P. Esselle, and A. Mehta, "Use of narrower reflection-canceling slots to design linearly polarized radial line slot arrays with improved radiation performance," *IEEE Antennas and Wireless Propagation Letters*, vol. 20, no. 12, pp. 2275–2279, 2021.

[33] J. I. Herranz-Herruzo, A. Valero-Nogueira, M. Ferrando-Rocher, and B. Bernardo-Clemente, "High-efficiency ka-band circularly polarized radial-line slot array antenna on a bed of nails," *IEEE Transactions on Antennas and Propagation*, vol. 70, no. 5, pp. 3343–3353, 2022.

[34] M. Bertrand, M. Ettorre, G. Valerio, M. Albani, and M. Casaletti, "A broadband low-profile circularly polarized radial line slot antenna," *IEEE Transactions on Antennas and Propagation*, vol. 71, no. 1, pp. 140–150, 2023.